Analysis of Interfacial Stresses of 3D Laminated Composites by a Regularized Boundary Integral Equation

Y. C. Shiah[1*]

[1] Department of Aeronautics & Astronautics, National Cheng Kung University, Tainan, Taiwan

* *Y. C. Shiah* (*ycshiah@mail.ncku.edu.tw)*

Keywords: *boundary element method; laminated composites; exponential transformation*

1. Abstract

In engineering applications, laminated composites have been widely applied in various disciplines. The structures are characterized by their thicknesses dimensioned with several orders below their characteristic length. For yielding reliable results by domain solution techniques (for example the finite element method), the "cell elements" employed must have proper aspect ratios that are normally greater than 1:20. Due to this aspect-ratio constraint, the domain modeling of laminates shall take tremendous amounts of elements, leading to overloading computations. As a powerful alternative of numerical modeling, the boundary element method (BEM) has been extensively applied for various engineering analyses for its major advantage of boundary modeling. However, another serious issue will arise in the modeling, that is the integration of nearly singular integrals. This problem occurs under the situation when the source-point on one side is very near the element of integration on its opposite side. This paper proposes an exponential transformation applied to regularize the nearly singular integrals in the 3D BEM-modeling of thin laminated composites. Through the transformation, the integrands will behave well without rapid fluctuations and thus, any regular numerical scheme of integration can be properly applied. This regularization process is implemented in the BEM to analyze the interfacial stresses of 3D laminated composites, where each layer is treated as a generally anisotropic material. In the end, a numerical example is presented, verified with ANSYS analysis.

Keywords: *boundary element method; laminated composites; nonlinear transformation*

2. Introduction

Thin layered composites are widely applied in engineering practice across various disciplines, such as fibre-reinforced polymers, laminated plates, and sandwich panels. Thin multi-layered composites usually consist of several thin layers of dissimilar materials bonded together with adhesives to improve their strength-to-weight ratios. Due to the mismatch in mechanical properties among the bonded materials, severe interlaminar stresses may arise, which can endanger the structural integrity of the composites. When manufacturing defects or voids are present at the interfaces, potential debonding or delamination becomes a major concern in the use of laminated composites. Although analytical approaches based on approximations can provide detailed insights, simulations under general conditions still require the use of numerical tools. Owing to its versatility, the finite element method (FEM) is widely adopted for such analyses. For instance, Ojo and Weaver [1] proposed a strong-form anisoparametric unified formulation that combines a cross-sectional finite element with a differential quadrature beam element to investigate this problem. Tian et al. [2] analysed stress distributions around cutouts in laminated composites using a hybrid stress multilayer approach based on two specialized finite element techniques. Employing a higher-order layer-wise theory, Li and Chen [3] developed a thermoelastic finite element model to examine laminated composite beams incorporating layers of active shape memory alloys. Ali et al. [4] introduced an efficient algorithm for finite element reliability analysis to predict the onset of edge delamination caused by interlaminar stresses. Furthermore, Santana et al. [5] conducted a comprehensive nonlinear finite element study of laminated shells, enabling accurate prediction of the behavior of laminated composite structures under progressive damage.

However, reliable FEM analysis requires appropriate aspect ratios of the modelling elements (or "cells") throughout the domain, commonly no more than 20:1. This requirement creates significant difficulty in modelling three-dimensional laminated composites, which often consist of several extremely thin laminates with dissimilar properties. Consequently, an overwhelming number of elements are needed for domain discretisation, leading to excessive computational cost. This issue becomes even more critical when modelling extremely thin adhesive layers (commonly using epoxy resin). For this reason, conventional FEM modelling often neglects the presence of adhesives. Nevertheless, delamination in composites usually occurs due to fracture of the adhesive layers at edges or defects along the interfaces. As a result, such omission therefore fails to provide an adequate assessment of the structural strength of laminated composites, being subjected to loading. Although the boundary element method (BEM) has been widely applied across various engineering disciplines, studies reporting its implementation for simulating interlaminar stresses in thin laminated composites remain extremely scarce. As a powerful alternative computational tool, the BEM is highly efficient for its boundary modelling only. This characteristic is particularly attractive for modelling thin laminated composites, where discretization of the internal thin layers is unnecessary. Nevertheless, this advantage was not exploited for modelling thin laminates until the pioneering work of Shiah and Hsu [6], who first reported a successful 2D implementation for thin laminated composites subjected to inertial loads. Although extending this 2D formulation to 3D may appear straightforward, the problem is considerably more intricate than it initially seems. The nasty issue lies in the proper evaluations of nearly singular integrals in 3D modelling when the source point on one side is very near the integration element on its opposite. Over the years, numerous regularization techniques for nearly singular integrals have been proposed, including distance transformation methods (e.g., [7–10]), non-linear transformations (e.g., [11–13]), analytical or semi-analytical algorithms (e.g., [14]), self-regularization approaches (e.g., [15, 16]), and SINH-transformations (e.g., [17, 18]). Nevertheless, none of these schemes have yet been implemented to address the specific problem of modelling 3D laminated composites investigated in this study.

This paper introduces a nonlinear transformation to regularize boundary integrals in the BEM for analysing interlaminar stresses in three-dimensional anisotropic composites. The regularization enables accurate modeling of three-dimensional laminated composites using very coarse meshes, even when extremely thin adhesive layers are included. Numerical examples demonstrate the effective implementation of the proposed approach for solving elastic problems in laminated composites. For validation, the layer thicknesses are selected to be compatible with finite element modeling, and the results are compared with simulations conducted using ANSYS.

3. Three-dimensional elastic analysis of the BEM

3.1. Boundary integral equation

As has been well established, the boundary integral equation relating the nodal values of displacements u_j and tractions t_j of the field point Q and the source point P on the surface Γ is expressed as

$$C_{ij}\, u_i = \int_S U_{ij} \cdot t_i \, d\Gamma - \int_S T_{ij} \cdot u_i \, d\Gamma , \tag{1}$$

where C_{ij} is the free coefficient at P; U_{ij} and T_{ij} are respectively the fundamental solutions of displacements and tractions in the x_i-direction at Q due to a unit load applied in the x_j-direction at P in an infinite elastic body. To model the multiple layers of laminated composites, the conventional sub-region technique is employed, in which both the displacements and tractions at the interface nodes are treated as unknowns. Applying the collocation procedure to each layer domain, auxiliary continuity conditions are imposed: equal displacements and opposite tractions at corresponding interface nodes. This leads to a square system of simultaneous equations that can be solved for all boundary unknowns. Because this sub-region process is standard, further procedural details are omitted. Each layer—whether an anisotropic laminate or an isotropic adhesive—is represented using its corresponding fundamental solutions. For angle-ply composite layers, only the principal material axis x_3, perpendicular to the plane of laminates, is rotated according to the ply orientation angle. For completeness, the fundamental solutions of anisotropic elastostatics are briefly summarized here.

For modelling thin layers of isotropic adhesive on interfaces, the fundamental solutions are given by

$$U_{ij}(P,Q) = \frac{\left[(3-4\nu)\delta_{ij} + r_{,i} r_{,j}\right]}{16\pi G(1\text{-}\nu) r}, \tag{2}$$

$$T_{ij} = \frac{-r_{,k} n_k \left[(1-2\nu)\delta_{ij} + 3 r_{,i} r_{,j}\right] - (1-2\nu)\left(r_{,i} n_j - r_{,j} n_i\right)}{8\pi(1-\nu) r^2}, \tag{3}$$

where all the parameters follow the usual notations, i.e. ν=Poisson’s ratio, G=shear modulus, and δ_{ij}= Kronecker Delta. In the above equations, r represents the geodesic distance between the source point P and the field point Q; n_i are components of the unit outward normal vector at the field point. When general anisotropy is considered, the corresponding fundamental solutions become mathematically more intricate. Detailed expressions of the anisotropic kernels can be found in [19], while only a brief overview of the formulations is provided here. The most expedient way for evaluating U_{ij} is to use the following analytical formulation,

$$\mathbf{U}(\mathbf{x})=\frac{1}{4\pi r}\frac{1}{|\boldsymbol{\kappa}|}\sum_{\mathbf{n}=0}^{4} q_n \hat{\boldsymbol{\Gamma}}^{(\mathbf{n})}\,, \tag{4}$$

where q_n are associated with the Stroh eigenvalues. As proposed in [19], Eq.(4) can be rewritten as a double Fourier series by the spherical coordinates (r, θ, ϕ) as follows:

$$U_{ij}(P,Q)=\frac{1}{4\pi r}\sum_{m=-\alpha}^{\alpha}\sum_{n=-\alpha}^{\alpha}\hat{\lambda}_{ij}^{(m,n)}\,\mathrm{e}^{\mathrm{i}(m\theta+n\phi)}\,, \tag{5}$$

where $\hat{\lambda}_{ij}^{(m,n)}$ are material constants to be determined by the standard Fourier analysis, carried out only once per BEM analysis regardless of how many elements/nodes are applied. In Eq. (5), α is an integer for the series to converge. Generally, α=12 is enough for general anisotropy. For evaluation of T_{ij}, the first-order derivatives of fundamental displacements are needed. For this purpose, spatial differentiations Eq. (5) are performed to give

$$U_{uv,l}=\frac{1}{4\pi r^2}\begin{cases}\displaystyle\sum_{m=-\alpha}^{\alpha}\sum_{n=-\alpha}^{\alpha}\hat{\lambda}_{uv}^{(m,n)}\mathrm{e}^{\mathrm{i}(m\theta+n\phi)}\begin{bmatrix}-\cos\theta\left(\sin\phi-\mathrm{i}\,n\cos\phi\right)\\ -\mathrm{i}\,m\sin\theta/\sin\phi\end{bmatrix} & \text{for } l=1\\ \displaystyle\sum_{m=-\alpha}^{\alpha}\sum_{n=-\alpha}^{\alpha}\hat{\lambda}_{uv}^{(m,n)}\mathrm{e}^{\mathrm{i}(m\theta+n\phi)}\begin{bmatrix}-\sin\theta\left(\sin\phi-\mathrm{i}\,n\cos\phi\right)\\ +\mathrm{i}\,m\cos\theta/\sin\phi\end{bmatrix} & \text{for } l=2\,.\\ \displaystyle\sum_{m=-\alpha}^{\alpha}\sum_{n=-\alpha}^{\alpha}\hat{\lambda}_{uv}^{(m,n)}\mathrm{e}^{\mathrm{i}(m\theta+n\phi)}\left[-\left(\cos\phi+\mathrm{i}\,n\sin\phi\right)\right] & \text{for } l=3\end{cases} \tag{6}$$

As usual for performing the collocation procedure, the boundary is discretized into M elements. By using the standard shape functions, denoted by N_c, to interpolate the displacements and tractions at Q, the discretized form of Eq. (1) is rewritten as

$$\begin{aligned}C_{ij}\,u_i=&\sum_{m=1}^{M}\sum_{c=1}^{8/6}t_i^{(c)}\int_{-1}^{1}\int_{-1}^{1}\left[N_c^{(8/6)}(\xi,\eta)\cdot U_{ij}(\xi,\eta)\cdot J(\xi,\eta)\right]d\xi\,d\eta\\ &-\sum_{m=1}^{M}\sum_{c=1}^{8/6}u_i^{(c)}\int_{-1}^{1}\int_{-1}^{1}\left[N_c^{(8/6)}(\xi,\eta)\cdot T_{ij}(\xi,\eta)\cdot J(\xi,\eta)\right]d\xi\,d\eta\end{aligned} \tag{7}$$

where $t_i^{(c)}$ / $u_i^{(c)}$ represent c-th nodal tractions/displacements of the element under integration. There are 8 /or 6 nodes per quadratic /or triangular element. In Eq. (7), (ξ,η) are the local intrinsic coordinates for transforming the Cartesian coordinates to the domain bounded by [1, 1] and $J(\xi,\eta)$ is the transformation Jacobian defined as usual. From Eqs. (5) and (6), it is apparent that **U** and **T** are characterized by the singular order O(1/r) and O(1/r^2), respectively. For brevity, the integrals in Eq. (7) are represented using

$$I_{ij}^{(c)}=\int_{-1}^{1}\int_{-1}^{1}\left[N_c^{(8/6)}(\xi,\eta)\cdot U_{ij}(\xi,\eta)\cdot J(\xi,\eta)\right]d\xi\,d\eta\,, \tag{8}$$

$$J_{ij}^{(c)} = \int_{-1}^{1}\int_{-1}^{1}\left[N_c^{(8/6)}(\xi,\eta)\cdot T_{ij}(\xi,\eta)\cdot J(\xi,\eta)\right]d\xi\, d\eta\,. \tag{9}$$

For illustrating the nearly singular nature of the both integrals in Eq. (8) and (9), the integrand of typical example is graphed in Fig. (1). Apparently, when the source point approaches the element, the integrand will rise rapidly near the projection point at (ξ_0,η_0) as illustrated in this figure. Any conventional scheme shall fail to properly evaluate the integral. The present work proposes an efficient transformation to regularize the nearly singular integrands such that conventional approaches can be applied for the integration.

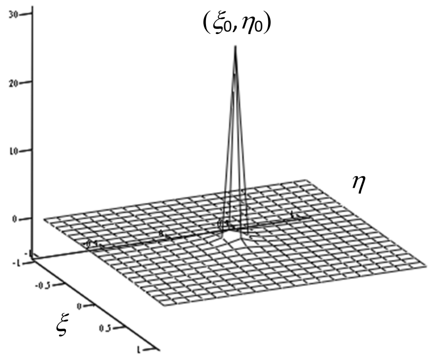

Figure 1: Integrand of a typical $I_{ij}^{(c)}$

3.2. *Regularization of integrals*

As explained above, the nastiest task to model 3D thin laminated composites is to properly evaluate the both integrals in Eq. (8) and Eq. (9) by conventional numerical schemes, for example the Gauss quadrature rule. When the source point approaches the element at an arbitrary inside point, the first task is to determine the projected coordinates (ξ_0,η_0). By interpolating the Cartesian coordinates of Q by the shape functions, the distance function is written as $R(\xi,\eta)$=$\sqrt{D(\xi,\eta)}$, where $D(\xi,\eta)$ is a quartic polynomial for quadratic elements. When the source point approaches the integration element, the minimum value will occur at $D(\xi_0,\eta_0)$. For the first guess, one may shoot an initial value $\eta^{(1)}$ and substitute it into the equation as follows:

$$\left.\frac{\partial D(\xi,\eta)}{\partial \xi}\right|_{\eta=\eta^{(1)}} = 0\,. \tag{10}$$

By numerically determining the real root of the cubic polynomial in Eq. (10), one obtains the corresponding $\xi^{(1)}$ as the first guessed value. Likewise, the 2nd shooting continues with

$$\left.\frac{\partial D(\xi,\eta)}{\partial \eta}\right|_{\xi=\xi^{(1)}} = 0\,, \tag{11}$$

which can be numerically solved for its real root, denoted by $\eta^{(2)}$. By repeating this procedure until convergent values at the n-th iteration are obtained, one may eventually determine the project point to be $(\xi_0,\eta_0)=(\xi^{(n)},\eta^{(n)})$. In principle, the integrands are monotonic, allowing for rapid convergence through the iterative procedure. When programming, it is useful to establish a criterion for triggering the regularization process when evaluating nearly singular integrals. The criterion can be as follows:

$$\varsigma = \left|D(\xi_0,\eta_0)\right| / D_{ave}\,, \tag{12}$$

where D_{ave} is the average value of $D(\xi,\eta)$ with all 8 nodal coordinates substituted in. For programming purposes, one can define a critical threshold of ς that triggers the regularization process. As a result, the projection distance to the element is thus given by $d = R(\xi_0,\eta_0)$. For the integrations, the domain bounded by [-1,1] is partitioned into four sub-domains at (ξ_0,η_0) as illustrated in Fig. 2. For performing the power-transformation, the following variable transformations for the m-th sub-element (m=1~4) need to be firstly defined,

$$u_m(s)=d\left[\left(1+\frac{A_m}{d}\right)^{\frac{s+1}{2}}-1\right],\quad v_m(s)=d\left[\left(1+\frac{B_m}{d}\right)^{\frac{t+1}{2}}-1\right],\tag{13}$$

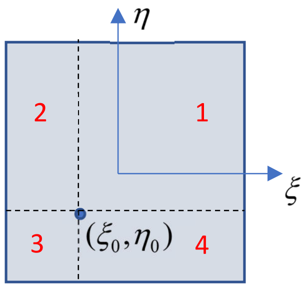

Figure 2: Partition of the domain

where (A_m, B_m) are given by

$$\left(A_m,B_m\right)=\begin{cases}\left(1,1\right) & \text{for } m\text{=1}\\ \left(1-\xi_0,1+\eta_0\right) & \text{for } m\text{=2}\\ \left(1+\xi_0,1-\eta_0\right) & \text{for } m\text{=3}\\ \left(1,1\right) & \text{for } m\text{=4}\end{cases}.\tag{14}$$

By transforming the local intrinsic coordinates $(\xi,\ \eta)$ into the new variables (s, t) as given in Eqs. (13), the integrals in Eq. (8) and Eq. (9) are rewritten as

$$I_{ij}^{(c)}=\sum_{m=1}^{4}\int_{-1}^{1}\int_{-1}^{1}\hat{U}_{ij}^{(c)}\left[u_m(s),v_m(t)\right]\hat{J}_m(s,t)\,ds\,dt\ ,\ J_{ij}^{(c)}=\sum_{m=1}^{4}\int_{-1}^{1}\int_{-1}^{1}\hat{T}_{ij}^{(c)}\left[u_m(s),v_m(t)\right]\hat{J}_m(s,t)\,ds\,dt\ ,\tag{15}$$

where $\hat{U}_{ij}^{(c)}, \hat{T}_{ij}^{(c)}$ are defined as follows:

$$\hat{U}_{ij}^{(c)}/\hat{T}_{ij}^{(c)}\left(u_m(s),v_m(t)\right)=\begin{cases}U_{ij}^{(c)}/T_{ij}^{(c)}\left(\text{-}u_m(s)+\xi_0,\text{-}v_m(t)+\eta_0\right) & \text{for } m\text{=1}\\ U_{ij}^{(c)}/T_{ij}^{(c)}\left(u_m(s)+\xi_0,\text{-}v_m(t)+\eta_0\right) & \text{for } m\text{=2}\\ U_{ij}^{(c)}/T_{ij}^{(c)}\left(\text{-}u_m(s)+\xi_0,v_m(t)+\eta_0\right) & \text{for } m\text{=3}\\ U_{ij}^{(c)}/T_{ij}^{(c)}\left(u_m(s)+\xi_0,v_m(t)+\eta_0\right) & \text{for } m\text{=1}\end{cases},\tag{16}$$

and the transformation Jacobian $\hat{J}_m(s,t)$ is given by

$$\hat{J}_m(s,t)=\frac{d^2}{4}\left(1+\frac{A_m}{d}\right)^{\frac{s+1}{2}}\left(1+\frac{B_m}{d}\right)^{\frac{t+1}{2}}\ln\left(1+\frac{A_m}{d}\right)\ln\left(1+\frac{B_m}{d}\right).\tag{17}$$

Through this transformation, rapid fluctuations of the nearly singular integrands will behave regularly such that the any conventional scheme may be applied to properly evaluate the integrals.

For illustrating the validity of this transformation, an example spherical element is considered, where the 8 nodes (c=1~8) are defined in the spherical coordinates (r_c, θ_c, ϕ_c) by

$$\begin{aligned} &r_i = 1, \quad \theta_1 = \theta_7 = \theta_8 = \pi/6, \quad \theta_2 = \pi/4, \quad \theta_3 = \theta_4 = \theta_5 = \pi/3, \quad \theta_6 = \pi/4, \\ &\phi_1 = \phi_2 = \phi_3 = \pi/3, \quad \phi_4 = \phi_8 = \pi/4, \quad \phi_5 = \phi_6 = \phi_7 = \pi/6. \end{aligned} \tag{18}$$

Suppose the source point is located very near the element at (r, θ, ϕ)=(1-10^{-6}, π/4, π/4). The mechanical constants are E=1000 (units), ν=0.3 by assumption. Via the iteration as described above, the projection coordinates (ξ_0, η_0) are determined to be (0, -2.2416643×10^{-3}). For numerical integrations of the transformed integrals, the Gauss quadrature rule using 18-point were applied. For verifications, the original integrals were also evaluated by the mathematical software MathCAD with default tolerance set to 10^{-12}. Table 1 shows the percentages of difference of the transformed approach when compared with the software computation using adaptive integration.

From the table, it is apparent that computations of the weakly singular integral $I_{ij}^{(c)}$ by the proposed transformation yield very accurate results totally agreeing with the software evaluations. For computations of the strongly singular one $J_{ij}^{(c)}$, the results are still accurate with minor difference. As can be seen from the comparison, the proposed transformation can accurately evaluate the nearly singular integrals even when the distance-ratio order is down to 10^{-6}. The order is considered sufficiently small indeed for modeling most engineering applications in practice. Next, successful implementation of the transformed approach will be illustrated by an example of a 3D laminated composite.

Table 1: Percentages of difference

c	$I_{ij}^{(c)}$	$J_{ij}^{(c)}$
1	$\begin{pmatrix} 0.00 & 0.00 & 0.00 \\ 0.00 & 0.00 & 0.00 \\ 0.00 & 0.00 & 0.00 \end{pmatrix}\%$	$\begin{pmatrix} 0.00 & 0.02 & 0.02 \\ 0.00 & 0.00 & 0.00 \\ 0.00 & 0.00 & 0.00 \end{pmatrix}\%$
2	$\begin{pmatrix} 0.00 & 0.00 & 0.00 \\ 0.00 & 0.00 & 0.00 \\ 0.00 & 0.00 & 0.00 \end{pmatrix}\%$	$\begin{pmatrix} 0.00 & 0.01 & 0.00 \\ 0.01 & 0.00 & 0.00 \\ 0.00 & 0.00 & 0.00 \end{pmatrix}\%$
3	$\begin{pmatrix} 0.00 & 0.00 & 0.00 \\ 0.00 & 0.00 & 0.00 \\ 0.00 & 0.00 & 0.00 \end{pmatrix}\%$	$\begin{pmatrix} 0.00 & 0.00 & 0.00 \\ 0.02 & 0.00 & 0.03 \\ 0.00 & 0.00 & 0.00 \end{pmatrix}\%$
4	$\begin{pmatrix} 0.00 & 0.00 & 0.00 \\ 0.00 & 0.00 & 0.00 \\ 0.00 & 0.00 & 0.00 \end{pmatrix}\%$	$\begin{pmatrix} 0.00 & 0.00 & 0.00 \\ 0.00 & 0.00 & 0.00 \\ 0.00 & 0.00 & 0.00 \end{pmatrix}\%$
5	$\begin{pmatrix} 0.00 & 0.00 & 0.00 \\ 0.00 & 0.00 & 0.00 \\ 0.00 & 0.00 & 0.00 \end{pmatrix}\%$	$\begin{pmatrix} 0.00 & 0.00 & 0.00 \\ 0.01 & 0.00 & 0.00 \\ 0.07 & 0.01 & 0.00 \end{pmatrix}\%$
6	$\begin{pmatrix} 0.00 & 0.00 & 0.00 \\ 0.00 & 0.00 & 0.00 \\ 0.00 & 0.00 & 0.00 \end{pmatrix}\%$	$\begin{pmatrix} 0.00 & 0.01 & 0.00 \\ 0.01 & 0.00 & 0.00 \\ 0.00 & 0.00 & 0.00 \end{pmatrix}\%$
7	$\begin{pmatrix} 0.00 & 0.00 & 0.00 \\ 0.00 & 0.00 & 0.00 \\ 0.00 & 0.00 & 0.00 \end{pmatrix}\%$	$\begin{pmatrix} 0.00 & 0.01 & 0.00 \\ 0.00 & 0.00 & 0.00 \\ 0.01 & 0.07 & 0.00 \end{pmatrix}\%$
8	$\begin{pmatrix} 0.00 & 0.00 & 0.00 \\ 0.00 & 0.00 & 0.00 \\ 0.00 & 0.00 & 0.00 \end{pmatrix}\%$	$\begin{pmatrix} 0.00 & 0.00 & 0.00 \\ 0.00 & 0.00 & 0.00 \\ 0.00 & 0.00 & 0.00 \end{pmatrix}\%$

4. Numerical example

The proposed approach has been implemented in an existing BEM code, developed for elastic analysis of generally anisotropic materials using quadratic isoperimetric elements. As shown in Fig. 3, this example treats a square angle-ply laminated composite (L×L) with 5 layers- [90°/45°/0°/45°/90°] subjected to biaxial tension P on surfaces B and C, while surface A and D are constrained in their normal directions.

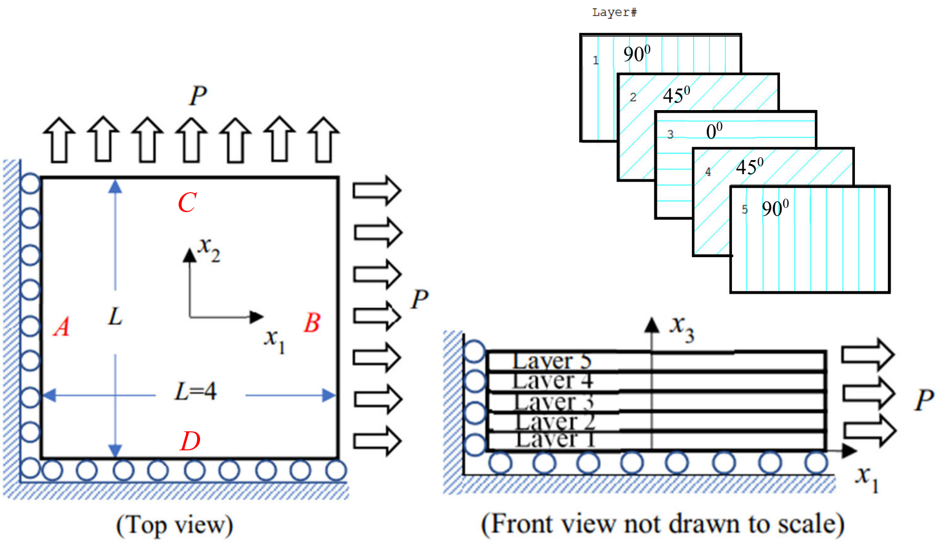

Figure 3: Angle-ply laminates subjected to biaxial tension

Additionally, the top surface is free of tractions and the bottom is constrained in the x_3-axis. For the analysis, glass/epoxy is chosen to be the material, having the properties:

$$\begin{aligned} &E_1{=}34.5\ \text{(GPa)}, E_2{=}51.6\ \text{(GPa)}, E_3{=}25\ \text{(GPa)},\\ &\nu_{12}{=}0.28,\ \nu_{23}{=}0.28, \nu_{13}{=}{=}0.34,\\ &G_{12}{=}3.7\ \text{(GPa)}, G_{23}{=}62\ \text{(GPa)}, G_{31}{=}6.3\ \text{(GPa)}. \end{aligned} \tag{19}$$

Thickness of each layer, t_0, is firstly taken to be $0.00025L$. For the BEM modeling, 800 quadratic elements with 2410 nodes were applied as shown in Fig. 4. For independent verification, analysis by ANSYS was also carried out, where 40000 SOLID186 elements with total 171011 nodes were applied (Fig. 4). For comparison, this BEM analysis was also conducted using the technique of self-regularization [16]. The calculated stresses σ_{11} and σ_{12} are plotted in Fig. 5 and Fig. 6, respectively. Obviously, for the distance ratio, the BEM by self-regularization fails to provide proper analysis, while the BEM analysis by transformation is consistent with the ANSYS results. In fact, this distance ratio has reached the limit of employing ANSYS for the analysis using our desktop PC. Despite the BEM analysis by transformation is still applicable for treating smaller thickness reliable ANSYS modeling would paralyze the simulation due to the overwhelming meshes required.

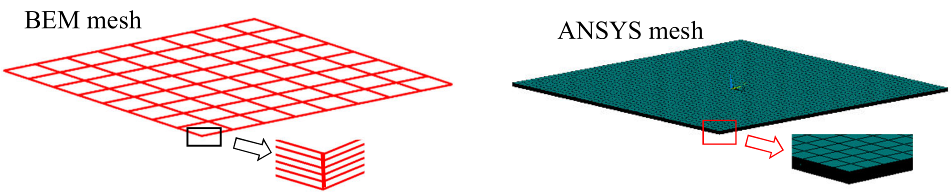

Figure 4: Modeling of the angle-ply laminates

5. Conclusions

A primary concern in laminated composites is the potential debonding, which typically initiates at the interfaces between layers. To ensure structural integrity, accurate and efficient evaluation of interlaminar stresses is essential. However, conventional domain-based solution techniques often struggle to provide reliable analyses, as modeling extremely thin layers requires an excessively refined mesh. In this paper, an efficient BEM framework is developed to analyze interlaminar stresses in laminated anisotropic composites using only coarse meshes. A key challenge in BEM—the evaluation of nearly singular integrals—is addressed through a nonlinear transformation. The numerical example indicates that the proposed BEM approach is highly suitable for investigating interlaminar stresses in 3D laminated composites.

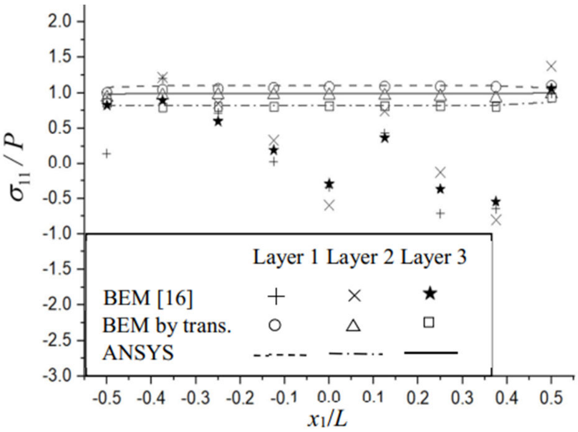

Figure 5: σ_{11} on surfaces along x_2=0

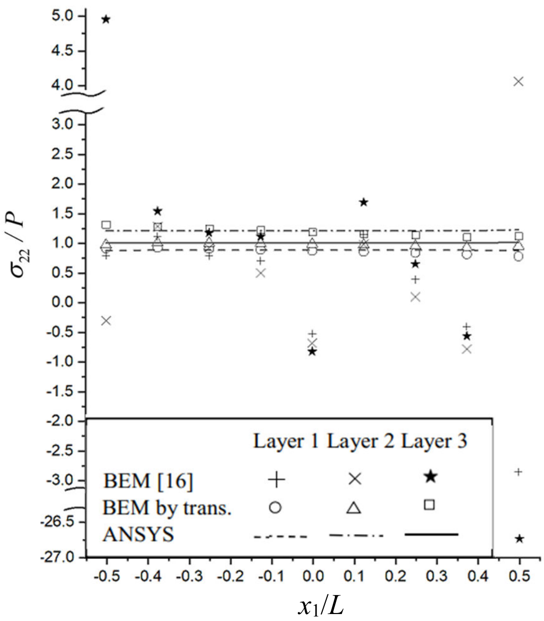

Figure 6: σ_{22} on surfaces along x_2=0

Acknowledgements

The financial support provided to the author from the National Science and Technology Council of Taiwan is greatly appreciated (114-2221-E-006 -072 -MY2).

6. References

[1] Ojo S.O., Weaver P.M., "Efficient strong unified formulation for stress analysis of non-prismatic beam structures". Compos Struct, Vol. 272, 114190, 2021.
[2] Tian Z-S, Yang Q-P, Wang A-P. "Three-dimensional stress analyses around cutouts in laminated composites by special hybrid finite elements". J Compos Mater Vol. 50, No.1, pp.75-98, 2016.
[3] Wei Li, Yuchen Chen. "Coupled higher-order layerwise mechanics and finite element formulations for laminated composite beams with active SMA layers". Eur J Mech A Solids, Vol. 107, 105380, 2024.
[4] Ali Delbariani-Nejad, Amin Farrokhabadi, Mohammad Fotouhi. "Finite element reliability analysis of edge delamination onset due to interlaminar stresses in composite laminates". Compos Struct, Vol. 288, 115410. 2022.

[5] Pedro Bührer Santana, António Joaquim Mendes Ferreira, Herbert Martins Gomes, Volnei Tita. “Nonlinear finite element damage analysis of laminated shells by Carrera Unified Formulation”. Compos Struct, Vol. 348, 118494, 2024.

[6] Y.C. Shiah, Kuo-Wei Hsu. “Two-dimensional analysis of interlaminar stresses in thin anisotropic composites subjected to inertial loads by regularized boundary integral equation”. Composites, Part B, Vol. 159, pp.105-113. 2019.

[7] Scuderi Letizia. “On the computation of nearly singular integrals in 3D BEM collocation”. *Internat J Numer Methods Engrg*, Vol.74, pp.1733-1770, 2007.

[8] H. Ma, N. Kamiya. “A general algorithm for the numerical evaluation of nearly singular boundary integrals of various orders for two- and three-dimensional elasticity”. *Comput Mech*, Vol. 29, pp. 277-288, 2002.

[9] H. Ma, N. Kamiya. “Distance transformation for the numerical evaluation of near singular boundary integrals with various kernels in boundary element method”. *Eng Anal Bound Elem*, Vol. 26, pp. 329-339. 2002.

[10] Xianyun Qin, Jianming Zhang, Guizhong Xie, Fenglin Zhou, Guanyao Li. “A general algorithm for the numerical evaluation of nearly singular integrals on 3D boundary element”. *J Comput Anal App*, Vol. 235, pp. 4174-4186, 2011.

[11] J.C.F. Telles. “A self-adaptive co-ordinates transformation for efficient numerical evaluation of general boundary element integrals”. *Internat J Numer Methods Engrg*, Vol. 24, pp. 959–973, 1987

[12] X.L. Chen, Y.J. Liu. “An advanced 3D boundary element method for characterizations of composite materials”. *Eng Anal Bound Elem*, Vol. 29, pp.513-523, 2005.

[13] K. Hayami. “Variable transformations for nearly singular integrals in the boundary element method”, *Publ Res Inst Math Sci*, Vol. 41, pp.821-842, 2005.

[14] Scuderi Letizia. “On the computation of nearly singular integrals in 3D BEM collocation”. *Internat J Numer Methods Engrg*, Vol. 74, pp.1733-1770, 2007.

[15] Y.C. Shiah, M.R. Hematiyan. “Interlaminar stresses analysis of three-dimensional composite laminates by the boundary element method”. *J Mech*, Vol. 34, pp.829-837, 2018.

[16] M.G He, C.L. Tan. “A self-regularization technique in boundary element method for 3-D Stress Analysis”. *CMES-Comput Model Eng Sci*, Vol. 95, pp. 317-349, 2013.

[17] B.M. Johnston, P.R. Johnston, D. Elliott. “A sinh transformation for evaluating two-dimensional nearly singular boundary element integrals”. *Internat J Numer Methods Engrg*, Vol. 69, pp.1460-1479, 2007.

[18] Xiaochao Li, Yu Su. “Three-dimensional stress analysis of thin structures using a boundary element method with sinh transformation for nearly singular integrals”. *Comput Math Appl*, Vol. 72, No.11, pp.2773-2787, 2016.

[19] Y.C. Shiah, C.L. Tan, and V.G. Lee. “Evaluation of Explicit-form Fundamental Solutions for Displacements and Stresses in 3D Anisotropic Elastic Solids”. CMES-Comp Model Eng Sci, Vol. 34, No. 3, pp.205-226, 2008.